Sound speed based patient-specific biomechanical modeling for registration of USCT volumes with X-ray mammograms

T. Hopp[a], A. Stromboni[a], N. Duric[b], M. Zapf[a], H. Gemmeke[a], N. V. Ruiter[a]

[a]Karlsruhe Institute of Technology, Institute for Data Processing and Electronics, Karlsruhe, Germany

[b]Barbara Ann Karmanos Cancer Institute, Department of Radiation Oncology, Detroit, USA

ABSTRACT

Ultrasound Computer Tomography is an upcoming imaging modality for early breast cancer detection. For evaluation of the method, comparison with the standard method X-ray mammography is of strongest interest. To overcome the significant differences in dimensionality and compression state of the breast, in earlier work a registration method based on biomechanical modeling of the breast was proposed. However only homogeneous models could be applied, i.e. inner structures of the breast were neglected. In this work we extend the biomechanical modeling of the breast by estimating patient-specific tissue parameters automatically from the speed of sound volume. Two heterogeneous models are proposed modeling a quadratic and an exponential relationship between speed of sound and tissue stiffness. The models were evaluated using phantom images and clinical data. The size of all lesions is better preserved using heterogeneous models, especially using an exponential relationship. The presented approach yields promising results and gives a physical justification to our registration method. It can be considered as a first step towards a realistic modeling of the breast.

Keywords: Sound Speed, Biomechanical Modeling, Registration, Ultrasound Computer Tomography, Mammography

1. INTRODUCTION

Ultrasound Computer Tomography (USCT) is an upcoming imaging modality for early breast cancer detection. It offers three-dimensional images of the breast in prone position.[1,2] The imaging method is based on numerous ultrasound transducers, which surround the breast within a water bath. Three types of images are provided: reflection, attenuation and speed of sound images. Reflection images reveal changes in the echotexture and are therefore able to image the surface of tissues. This results in the visualization of the morphology of the tissue. Attenuation and especially speed of sound images are expected to provide tissue characterization.[3] A high speed of sound and a high attenuation compared to surrounding tissue might be an indicator of cancerous tissue. Furthermore also fatty and fibroglandular tissue can be distinguished by the attenuation and speed of sound information.[4] All three modalities are usually fused to display the breast architecture, parenchyma and suspicious lesions simultaneously.[5]

In order to evaluate the new imaging modality, comparison and correlation with the standard screening method X-ray mammography is of strong interest. X-ray mammography provides high resolution images and is capable of visualizing e.g. microcalcifications. However X-ray frequently provides poor contrast of tumors located within glandular tissue and only displays a projection image of the breast under compression. In clinical routine often additional imaging methods like Magnetic Resonance Imaging (MRI) are used for definite diagnosis. As such, USCT and X-ray mammography may be used in combination for a multimodal diagnosis in future. Especially for dense tissue, characterization by attenuation and speed of sound images may provide a guidance for diagnosis of cancerous lesions. In contrast to MRI, USCT does not need contrast agent to be administered to the patient for lesion vasculature visualization and is expected to be far less expensive.

Torsten Hopp, torsten.hopp@kit.edu, phone +49 721 608 2 5990, adress: Hermann-von-Helmholtz-Platz 1, Eggenstein-Leopoldshafen 76344, Germany, http://www.ipe.kit.edu/

Medical Imaging 2013: Ultrasonic Imaging, Tomography, and Therapy, edited by Johan G. Bosch, Marvin M. Doyley,
Proc. of SPIE Vol. 8675, 86750L · © 2013 SPIE · CCC code: 1605-7422/13/$18 · doi: 10.1117/12.2006726

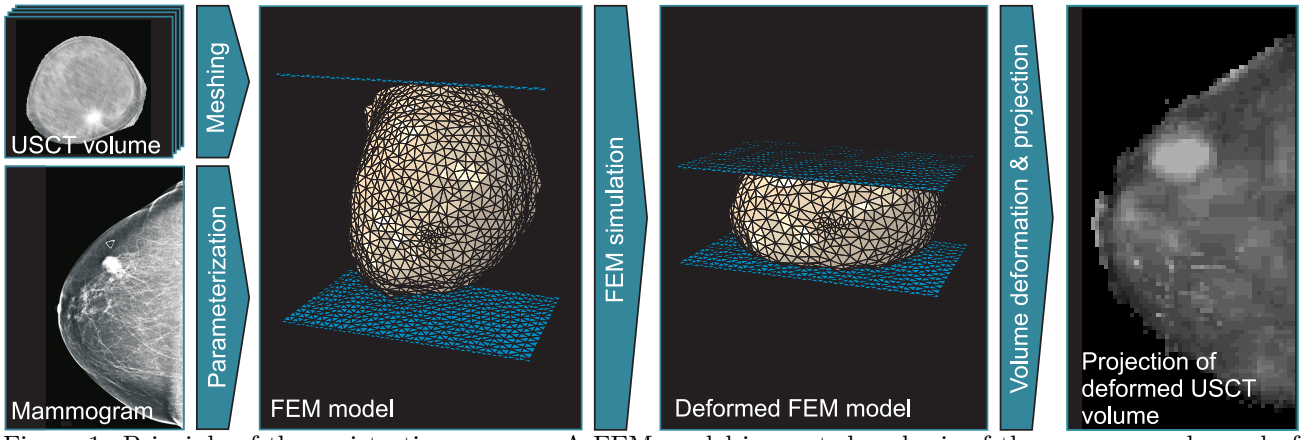

Figure 1: Principle of the registration process. A FEM model is created on basis of the preprocessed speed of sound volume using a meshing algorithm. The model is parameterized by information from the X-ray mammogram. Afterwards the compression simulation is carried out. Based on the deformed FEM model, the speed of sound volume is deformed and projected creating an image which is directly comparable to the X-ray mammogram.

The correlation between volume modalities like USCT and X-ray mammograms, however, is challenging and time consuming due to the different dimensionality of images, different patient positioning and different deformation state of the breast. We previously presented a registration and image fusion method[6–8] for comparison of USCT images and X-ray mammograms as well as for an efficient combined diagnosis with images of both modalities. The method is based on a patient-specific biomechanical model to simulate the huge deformation which is applied to the breast during mammography (Figure 1). The model is described as Finite Element Model (FEM) and built based on the USCT volume images. The FEM simulation then mimics the mammographic compression resulting in similar configurations of the USCT volume images as in a corresponding mammogram. The projection of this registered USCT volume image shows overlaying circumferences with the mammogram. Hence, both modalities can be compared directly and overlay images on mammograms for combined intuitive visualization can be created.[7]

Until now the applied biomechanical model was assumed to consist of homogeneous tissue, i.e. each Finite Element in the model was assigned the same material properties. The material properties were retrieved from literature and were constant for all patients. Internal structures of the breast like the fibroglandular tissue or different material properties for suspicious lesions were not considered until now. Hence, the deformable behavior of the breast was significantly simplified. This resulted amongst other things in a considerable increase of the lesion size in the projection image of the registered USCT dataset due to the compression simulation. In this work we extend the biomechanical modeling of the breast by estimating patient-specific tissue parameters automatically from the speed of sound volume to overcome the shortcomings of homogeneous models, in particular the lesion size increase in projection images of registered volumes.

2. METHODS

The challenge of the image registration is that X-ray mammograms are two-dimensional projections of the breast in a deformed configuration whereas the USCT volumes present the three-dimensional undeformed breast. The basic idea of our registration approach is to simulate the mammographic compression in order to achieve a deformed configuration of the USCT volume.[9] A projection of the deformed USCT volume in mammographic projection direction is then directly comparable to the X-ray mammogram (Figure 1). The compression is simulated using a biomechanical FEM model, which is built up based on the speed of sound volume. The registration is carried out in several processing steps. In the following subsections the main steps are presented.

2.1 Image preprocessing

The first step of the processing chain is the preprocessing of the speed of sound volumes and the mammograms. The mammograms are scaled to meet the resolution of the speed of sound volume. Rotations are performed to match the internally used coordinate system. Afterwards images are segmented to separate the breast boundary from the background. For the speed of sound images an automated presegmentation is carried out by the Karmanos Cancer Institute, Detroit.[10] Thresholding and morphological operations are applied to segment the mammogram.

2.2 Construction of the biomechanical model

Based on the preprocessed speed of sound volume, the patient-specific biomechanical model is built up. To describe the geometry of the model, a meshing algorithm[11] is applied, which divides the speed of sound volume into approximately 20,000 tetrahedral finite elements (FE). An adaptive meshing is used, i.e. the element size depends on the curvature of the surface of the breast.

The behavior of the model under compression depends on the underlying material model. We assume the breast tissue to be an incompressible material resulting in only a shape change, not in a change of volume. The incompressibility is approximated by a Poisson's ratio near 0.5. The stress-strain relationship of the breast tissue is described by an isotropic hyperelastic neo-hookean material model. For each Finite Element, the Young's modulus has to be defined. In earlier work, the values were obtained from literature, e.g. *Wellman et al.*,[12] *Samani et al.*,[13] *Krouskop et al.*,[14] assuming a homogeneous material equal to fatty tissue. However, different types of tissue are expected to have different material properties. This especially holds for lesions which have an increased stiffness compared to surrounding tissue. The increased stiffness of hard tumors results in a preservation of the lesion shape. Therefore a compression neglecting stiffness differences in tissue like the model used in our earlier work results in a change of the lesion size in a projection image. In this work we use the speed of sound distribution in the breast, to estimate the material parameters, i.e. the stiffness of the tissue expressed by the Young's modulus, of the biomechanical FEM model.

For each Finite Element the mean speed of sound is calculated from the quantitative speed of sound volume. The intensities of voxels, i.e. the speed of sound values, within a Finite Element are averaged. Afterwards the specific Young's modulus of the particular Finite Element is calculated. This calculation is carried out by the relationship between speed of sound c and Young's modulus E (equation (1))[15] in fluids. A constant density ρ from literature[16] and a constant Poisson's ratio ν are assumed. This model is referred to as heterogeneous model 1 throughout the paper.

$$E = 3\left(c^2\rho\right)(1-2\nu) \tag{1}$$

Equation (1) implies a quadratic relationship between c and E. However in literature exponential increase of stiffness from fatty over glandular to tumorous tissue is often measured.[12–14] To account for this behavior, additional material models were created by fitting an exponential function with supporting points at speed of sound values of $1.3\,km/s$ respectively $1.6\,km/s$. E at $1.3\,km/s$ was calculated using eq. 1, E at $1.6\,km/s$ was modeled to be five (heterogeneous model 2A), ten (heterogeneous model 2B) and 20 (heterogeneous model 2C) times higher than at $1.3\,km/s$. The relationship between c and E is illustrated in Figure 2 for each of the proposed models.

2.3 Registration

To simulate the compression of the breast during X-ray mammography, boundary conditions are formulated via parameterization of the model by information obtained from the mammogram. The mammographic compression is mimicked by a two step approach. In the first step, compression plates modeled as a acrylic glass like material are added to the simulation. They are moved closer until the thickness of the breast recorded during the X-ray mammography examination is reached. The interface between breast and plate is modeled without friction. Due to simplifications and uncertainties, images do not overlap congruently after carrying out the first simulation step. Hence the second step compensates the deviation between deformed volume image and the mammogram. For this purpose a target model is built up based on the segmented mammogram and displacement vectors between

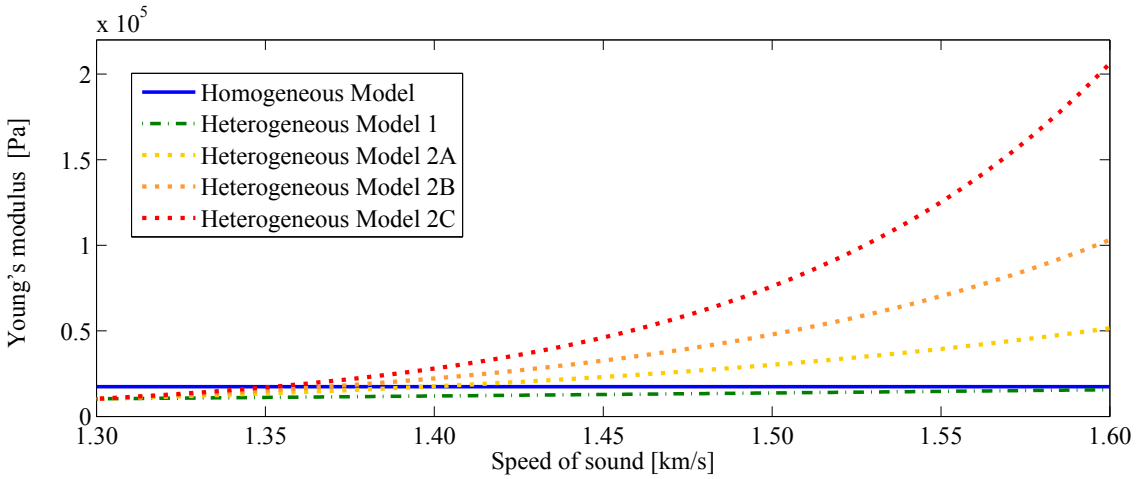

Figure 2: Relationship between sound speed and Young's modulus for the homogeneous and proposed heterogeneous models.

the deformed volume image after the first simulation step and the target model are defined on closest point basis.[17] The displacement vectors are applied as new boundary conditions. All FEM simulations are carried out using Abaqus.[18] More details on the registration process can be found in our earlier publications.[6–8,17]

3. RESULTS

3.1 Evaluation with phantom images

The effect of the proposed tissue models on the compression simulation was tested with phantom images. A semi-sphere was used to approximate the breast. Within the sphere three types of tissue were modeled: fatty tissue ($1.35\,km/s$), glandular tissue ($1.45\,km/s$) and tumorous tissue ($1.55\,km/s$). The size and position of the lesion was varied. Furthermore phantom simulations were carried out with and without glandular tissue. The models were compressed to 50% in thickness in the cranio-caudal direction using the first simulation step, i.e. compression plates were modeled and moved together to compress the phantom. Resulting images are shown in Figure 3.

To evaluate the effect of the mammographic compression on the lesion size, the size change of the included lesion in mediolateral and anteroposterior direction (Fig. 3) was analyzed. The lesion size in anteroposterior direction increased to an average of 133% using the homogeneous model and to 129% using the heterogeneous model 1. For the heterogeneous models 2A, 2B and 2C the size increased to 125%, 121% and 119% respectively.

In the mediolateral direction, the size changed to 114% using the homogeneous model, to 113% using the heterogeneous model 1 and to 110%, 110% and 108% using the heterogeneous models 2A, 2B and 2C respectively. Overall, the mediolateral expansion of the lesion is smaller as the expansion in anteroposterior direction. Lateral lesions are less expanded than central lesions. The lesion size is considerably better preserved using the exponential material models 2A, 2B and 2C. The overall breast size after compression varies by approximately 1% in each direction of space, i.e. mostly the internal structures are affected by the compression simulation.

To estimate the scale of the error which can be expected during the compression plate simulation with different material models, the centers of the modeled lesions after compression were compared. As a fixed reference the homogeneous model was used. The displacement between this reference point and the center point of the lesions compressed using the proposed heterogeneous material models was calculated by the three-dimensional Euclidean distance. The mean displacement was $0.5\,mm$ for the heterogeneous model 1, $1.1\,mm$ for the heterogeneous model 2A, $1.4\,mm$ for the heterogeneous model 2B and $2.2\,mm$ for the heterogeneous model 2C. The deviations are slightly higher for lateral lesions compared to central lesions as well as for smaller lesions compared to larger lesions.

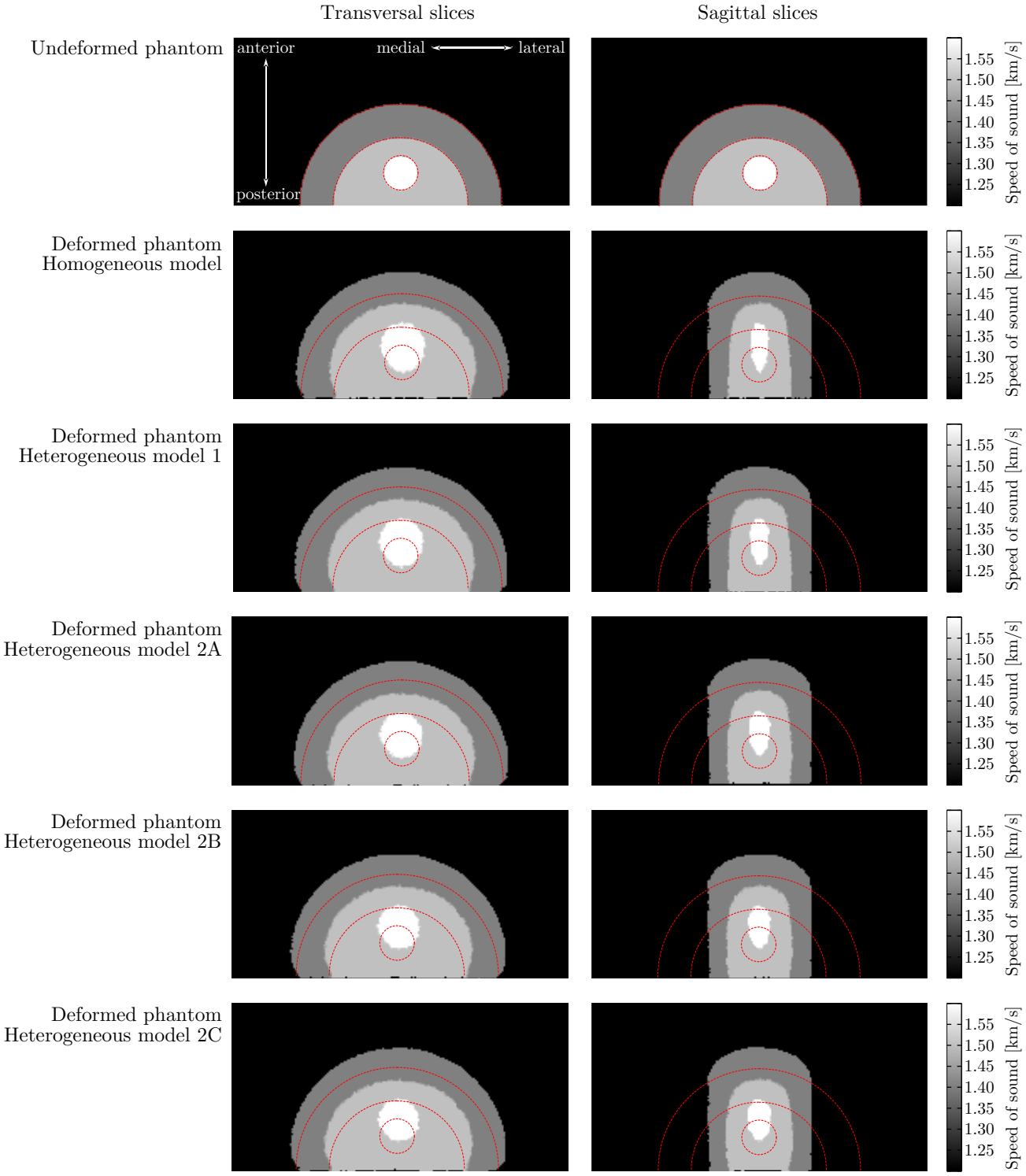

Figure 3: Transversal (each left) and sagittal (each right) slice images of the uncompressed phantom (top row) and the compressed phantoms using the homogeneous model, respectively the proposed heterogeneous models (Model 1, 2A, 2B, 2C). The phantoms contain three different structures mimicking fatty tissue (1.35 km/s, dark gray), glandular tissue (1.45 km/s, light gray) and lesion (1.55 km/s, white). The red dotted lines delineate the boundaries of the tissue before applying the compression simulation.

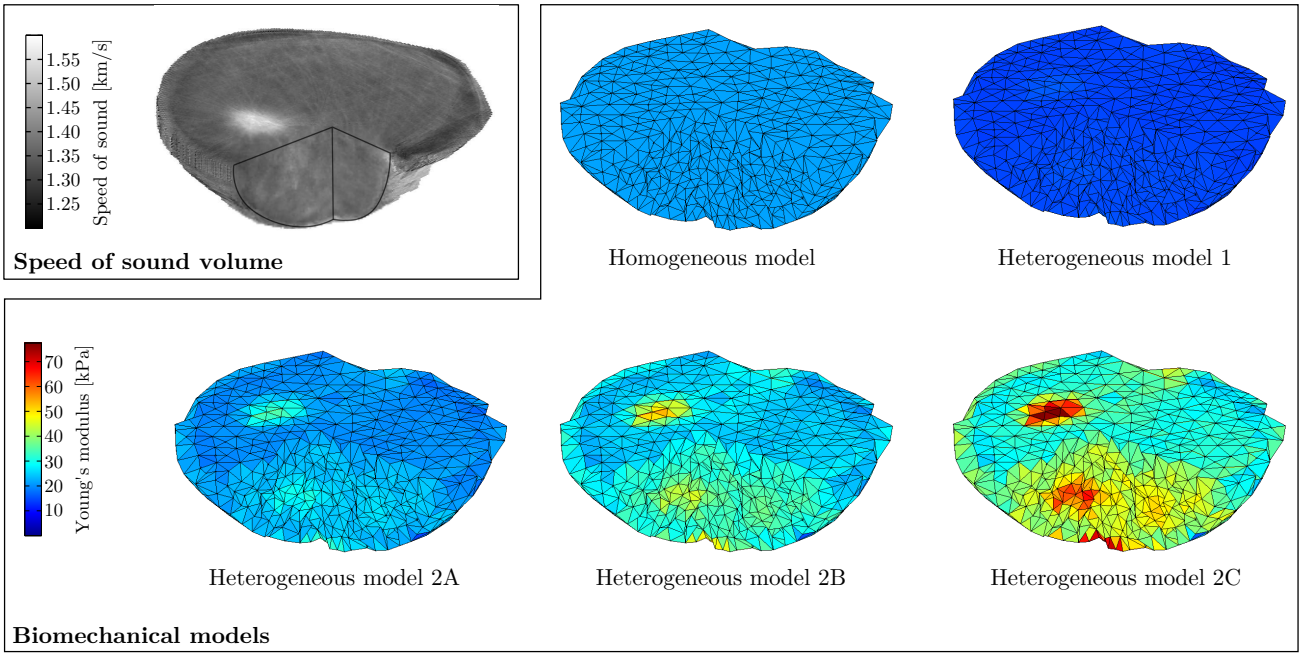

Figure 4: Biomechanical models built up based on the SOS volume of an exemplary patient using the proposed material models. Cut-open rendering of the SOS volume (top left) and cut-open FEM models.

3.2 Results with clinical images

After carrying out the phantom image evaluation, the sound speed based biomechanical modeling was applied to the registration of five clinical datasets from a clinical study at Karmanos Cancer Institute. Each dataset includes a volume image of each USCT modality (speed of sound, attenuation, reflectivity) and the corresponding craniocaudal mammogram. Digital as well as analog mammograms were used. The USCT volume images have a resolution of 1 mm. The spacing between the slices is 1 mm, the slice thickness is 4 mm. The number of slices varies depending on the size of the patient's breast.

The clinical datasets were chosen to show a lesion in the X-ray mammogram as well as in the USCT volume for evaluation purposes. After finishing the registration, a projection image of the resulting registered USCT volume was compared to the corresponding mammogram. The lesions in both images were marked by an expert and used as landmarks to determine the target registration error (TRE), which was calculated as the euclidean distance between the center points of the lesions.

The biomechanical models were built up according to the method described in section 2.2. Afterwards the registration process according to the method described in section 2.3 was conducted. The heterogeneous material models were applied in the first registration step, i.e. for the compression plate simulation which aims to mimic the breast compression realistically. For one typical case, the resulting biomechanical FEM models are illustrated in Figure 4. In all cases, the registration was performed successfully, i.e. there were no convergence problems of the FEM simulations due to the heterogeneous biomechanical models.

The mean TRE varied slightly for the different material models. Using the homogeneous model, a mean TRE of 12.2 mm (Median: 11.5 mm) was obtained. For the heterogeneous model 1 11.8 mm (Median 11.6 mm) could be observed and for the heterogeneous models 2A, 2B and 2C the mean TRE was 13.1 mm (Median 12.2 mm), 13.1 mm (Median 12.4 mm) and 12.1 mm (Median 11.9 mm) respectively. The standard deviation (SD) of the TRE between the different material models was in average 1.5 mm. The variations of the TRE for the different material models are predominantly caused by the second simulation step, i.e. the target model simulation. This becomes clear by evaluating the variations of the TRE after the first plate compression step in which the heterogeneous models were applied: the SD of the TRE between the different material models after this registration step was 0.3 mm.

Because of the different imaging methods, lesions may be represented differently in X-ray mammograms and speed of sound images. Furthermore the lesion marking is subject to an inter- and intraobserver variance. Consequently the marking of the lesion sizes in both imaging methods can not be compared directly. However comparing the size of the lesions in the speed of sound volume after applying the compression plate simulation with the size of the lesion in the X-ray mammogram gives an approximation of the relative lesion change caused by the heterogeneous modeling of the breast. The lesion size difference is in average reduced in mediolateral direction from 10.2 mm (homogeneous model) to 10.1 mm (heterogeneous model 1) respectively 9.9 mm, 9.8 mm, 9.5 mm (heterogeneous model 2A, 2B, 2C). In anteroposterior direction the difference decreased from 10.1 mm (homogeneous model) to 10.0 mm (heterogeneous model 1) respectively 9.9 mm, 9.9 mm, 9.8 mm (heterogeneous model 2A, 2B, 2C). The relative decrease of the lesion size in the projection image is approximately preserved during the second simulation step, i.e. for all heterogeneous models the difference in anteroposterior as well as in mediolateral direction is lower compared to the homogeneous model after the target model simulation step was performed. In consequence regions of high speed of sound in the final registered images (Figure 5) appear sharper, i.e. the lesion is less spread out.

Similarly to the evaluation using the phantom images, also the relative size changes of the lesions were evaluated. A threshold of 1.5 km/s was applied to the maximum intensity projections of the registered volumes to get a rough approximation of the lesion boundaries. Afterwards the lesion area was calculated by counting the number of pixels within the region (Figure 5). The area of the lesion after applying the complete registration with both simulation steps using the homogeneous model was set as a fixed reference. The lesion size was in average changed to 101% using the heterogeneous model 1, to 90% using the heterogeneous model 2A, to 89% using the heterogeneous model 2B and to 92% using the heterogeneous model 2C.

4. DISCUSSION AND CONCLUSION

After promising results in our earlier studies,[6–8] we extended our registration method by a physically reasonable biomechanical modeling of the breast. For the first time, an automatic patient specific biomechanical modeling based on the speed of sound distribution in the breast has been implemented. This allows for a more realistic modeling of the inner breast structures without using manual knowledge acquisition, e.g. no lesion annotation of a radiologist is needed to model increased tumor stiffness. The model has been integrated into our existing registration framework allowing for further investigation.

In this paper we evaluated the biomechanical modeling by phantom images as well as with clinical datasets. The phantom image evaluation shows the overall influence of using a heterogeneous material model in out registration method. A main observation is the decrease of the lesion size a projection image of the registered volume dataset using a higher stiffness at breast regions in which an enhanced speed of sound could be recognized. The exponential material models 2A, 2B and 2C preserve the lesion size slightly better than the heterogeneous model 1, which expresses a quadratic relationship between speed of sound and Young's modulus. Though mostly inner structures of the breast are affected by the compression simulation with heterogeneous material models, the registration error change caused by the material model is relatively low compared to other influencing factors evaluated in earlier studies.[19]

A similar behavior of the registration method can be observed for clinical datasets. While the effect of a heterogeneous material model on the target registration error is relatively low, the lesion size is better preserved in the final projection images. The effect of a heterogeneous material model might be enhanced using a more detailed modeling, e.g. by applying a FEM mesh with higher density and enhancing the resolution of the speed of sound images to image more details within the breast. The additional application of an anisotropic material behavior might be used to compensate for the macroscopic anisotropy of the breast under compression[20] without the need for a modeling of small inner structures like Cooper's ligaments. Such a patient-specific breast model obtained automatically from the speed of sound images might eliminate our second simulation step, which corrects for uncertainties in the compression plate simulation.

The automatic speed of sound based biomechanical modeling gives a physical justification to our registration method and can be considered as a first step towards a realistic modeling of the breast. All applied FEM simulations with phantom as well as with real data converged successfully. Despite of the small effect of the

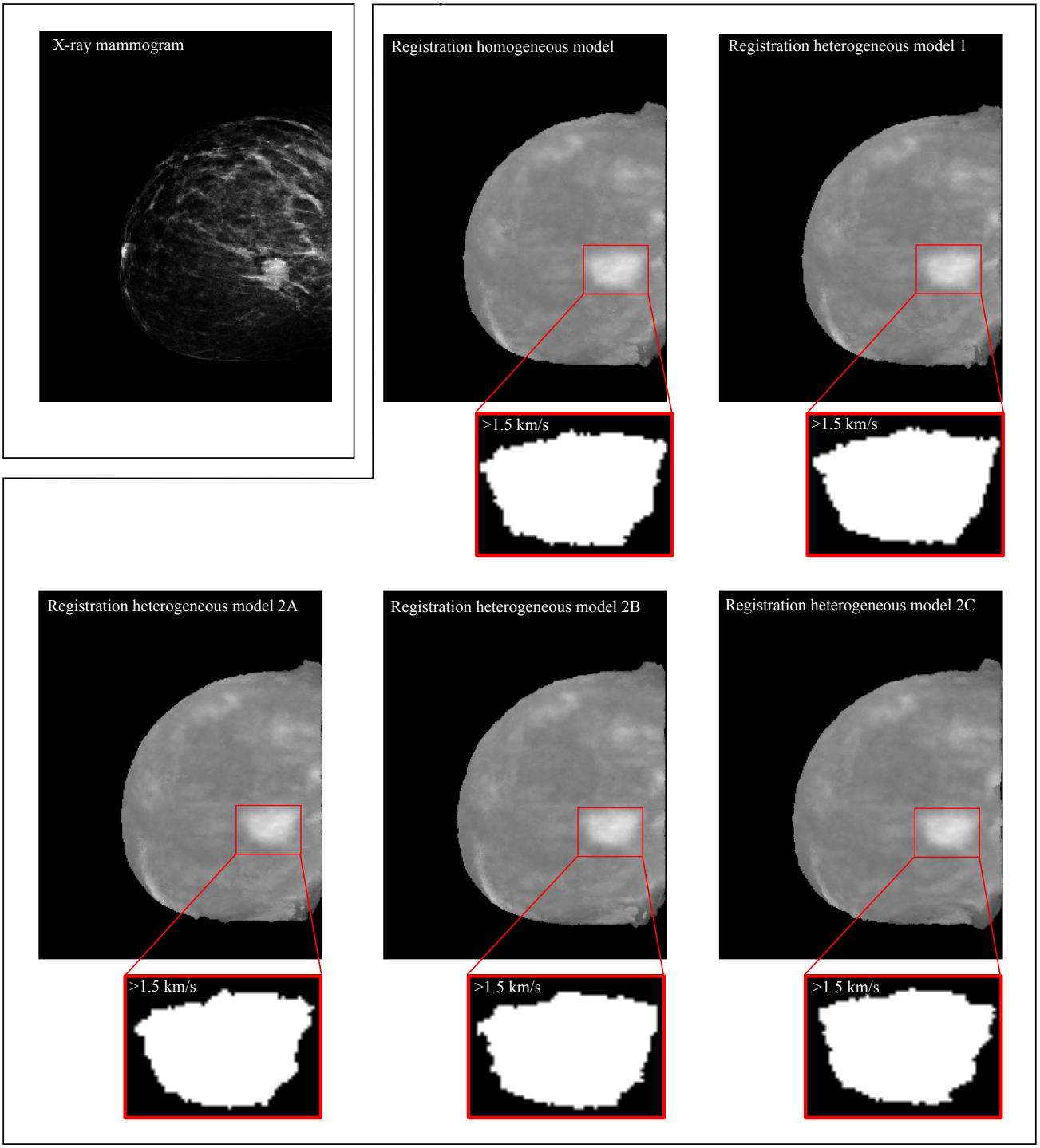

Figure 5: Resulting images of the registration: X-ray mammogram (top left) and maximum intensity projections of the registered speed of sound volumes using the proposed models. The enlarged images depict the lesion thresholded at a speed of sound of 1.5 km/s.

different material models on the registration error, the results are promising since the lesion size is better preserved, especially using the heterogeneous exponential models 2A, 2B and 2C). Our current research focuses on the application of the method to a larger clinical dataset and in-depth evaluation of applied material and registration parameters.

REFERENCES

[1] Duric, N., Littrup, P., Poulo, L., Babkin, A., Pevzner, R., Holsapple, E., Rama, O., and Glide, C., "Detection of breast cancer with ultrasound tomography: First results with the computerized ultrasound risk evaluation (C.U.R.E)," *Medical Physics* **34**(2), 773–785 (2007).

[2] Gemmeke, H. and Ruiter, N., "3d ultrasound computer tomography for medical imaging," *Nuclear Instruments and Methods in Physics Research Section A: Accelerators, Spectrometers, Detectors and Associated Equipment* **580**(2), 1057 – 1065 (2007).

[3] Greenleaf, J. F. and Bahn, R. C., "Clinical imaging with transmissive ultrasonic computerized tomography," *Journal of Computer Assisted Tomography* **5**(5), – (1981).

[4] Hopp, T., Duric, N., and Ruiter, N., "Breast tissue characterization by sound speed: Correlation with mammograms using a 2d/3d image registration," in [*Proceedings 2012 IEEE International Ultrasonics Symposium (IUS)*], (2012).

[5] Duric, N., Littrup, P., Chandiwala-Mody, P., Li, C., Schmidt, S., Myc, L., Rama, O., Bey-Knight, L., Lupinacci, J., Ranger, B., Szczepanski, A., and West, E., "In-vivo imaging results with ultrasound tomography: report on an ongoing study at the karmanos cancer institute," in [*Proceedings SPIE Medical Imaging*], **7629**(1), 76290M (2010).

[6] Hopp, T., Holzapfel, M., Ruiter, N. V., Li, C., and Duric, N., "Registration of X-ray Mammograms and Three-Dimensional Speed of Sound Images of the Female Breast," in [*Proceedings SPIE Medical Imaging*], **7629**(1), 762905 (2010).

[7] Hopp, T., Bonn, J., Ruiter, N. V., Sak, M., and Duric, N., "2D/3D Image Fusion of X-ray Mammograms with Speed of Sound Images: Evaluation and Visualization," in [*Proceedings SPIE Medical Imaging*], **7968**(1), 79680L (2011).

[8] Hopp, T., Duric, N., and Ruiter, N., "Automatic Multimodal 2D/3D Image Fusion of Ultrasound Computer Tomography and X-ray Mammography for Breast Cancer Diagnosis," in [*Proceedings SPIE Medical Imaging*], **8320**(1), 83200P (2012).

[9] Ruiter, N. V., Stotzka, R., Mueller, T. O., Gemmeke, H., Reichenbach, J. R., and Kaiser, W. A., "Model–based registration of x–ray mammograms and mr images of the female breast," *IEEE Transactions on Nuclear Science* **53**, 204 – 211 (2006).

[10] Sak, M., Duric, N., Boyd, N., Littrup, P., West, E., and Li, C., "Breast tissue composition and breast density measurements from ultrasound tomography," in [*Proceedings SPIE Medical Imaging*], **8320**(1), 83200Q (2012).

[11] Fang, Q. and Boas, D., "Tetrahedral mesh generation from volumetric binary and grayscale images," *IEEE International Symposium on Biomedical Imaging: From Nano to Macro, 2009. ISBI '09.* , 1142 –1145 (2009).

[12] Wellman, P. S., Howe, R. D., Dalton, E., and Kern, K. A., "Breast tissue stiffness in compression is correlated to histological diagnosis," technical report, Harvard BioRobotics Laboratory (1999).

[13] Samani, A., Zubovits, J., and Plewes, D., "Elastic Moduli of Normal and Pathological Human Breast Tissues: an Inversion-Technique-Based Investigation of 169 Samples," *Physics in Medicine and Biology* **52**(6), 1565–1576 (2007).

[14] Krouskop, T. A., Wheeler, T. M., Kallel, F., Garra, B. S., and Hall, T., "Elastic Moduli of Breast and Prostate Tissues Under Compression," *Ultrasonic Imaging* **20**, 260–274 (1998).

[15] Young, D., Munson, B., Okiishi, T., and Huebsch, W., [*A Brief Introduction To Fluid Mechanics*], John Wiley & Sons (2010).

[16] J.H. Hubbell, S. S., "Table of x-ray mass attenuation coefficients and mass energy-absorption coefficients from 1kev to 20 mev for elements z=1 to 92 and 48 additional substances of dosimetric interest," tech. rep., National Institute of Standards and Technology, Gaithersburg, MD (2004). Online Available: http://physics.nist.gov/xaamdi.

[17] Hopp, T., *Multimodal Registration of X-Ray Mammograms with 3D Volume Datasets*, PhD thesis, University of Mannheim (2012).
[18] Dassault Systmes, *Abaqus 6.11 Online Documentation* (2011).
[19] Hopp, T. and Ruiter, N., "Configurable Framework for Automatic Multimodal 2D/3D Registration of Volume Datasets with X-Ray Mammograms," in [*Proceedings of the Workshop on Breast Image Analysis in conjunction with MICCAI 2011*], 161–168 (2011).
[20] Tanner, C., White, M., Guarino, S., Hall-Craggs, M., Douek, M., and Hawkes, D., "Anisotropic behaviour of breast tissue for large compressions," in [*IEEE International Symposium on Biomedical Imaging 2009: From Nano to Macro*], 1223 –1226 (2009).